Indus Journal of Social Sciences

Online ISSN: 2960-219X
Print ISSN: 2960-2203
Volume 3, Number 2, 2025, Pages 151 – 168
Journal Home Page
https://induspublishers.com/IJSS/about

Geo-Spatial Evolution of Desertification in Cholistan Desert of South Punjab, Pakistan

Muhammad Zulqadar Faheem[1], Muhammad Farrukh Shahzad[2], Muhammad Waseem Iqbal[3] & Muhammad Asif[4]

[1,4]*Department of Geography, The University of Karachi, Pakistan*
[2,3]*Government College University of Faisalabad, Pakistan*

ARTICLE INFO

Article History:

Received:	*February*	*20, 2025*
Revised:	*April*	*04, 2025*
Accepted:	*April*	*06, 2025*
Available Online:	*April*	*09, 2025*

Keywords:

Landsat, Maximum likelihood classification, NDVI, NDBaI, Arid ecosystem

Corresponding Author:
Muhammad Zulqadar Faheem
Email:
zulqadarf@gmail.com

ABSTRACT

Satellite remote sensing has become a dependable geospatial technology for accurately evaluating land use and land cover across global, regional or local scales. This research aims to assess changes in land cover and land use in the Cholistan Desert through Supervise classification and NDVI, NDbaI and TGSI indices, which is located in southern Punjab, Pakistan. Landsat data has been a reliable source for historical images of the Earth's surface over the past 25 years due to its consistency and practicality. The present research utilizes satellite data from Landsat 5 TM for the years 1996, 2002, and 2008, along with Landsat 8 OLI for the years 2014 and 2020. To calculate the area percentage, change and annual dynamic rate of change at discrete time intervals, maximum likelihood supervised classification and change detection algorithms are necessary. In this work, the methods employed for change detection utilize remote sensing indices like the normalized difference vegetation index, the top grain soil index, and the normalized difference bareness index. Between 1996 and 2020, the findings show that agricultural land grew at a rate of 2.3%, while uncultivated land diminished at a dynamic rate of 0.5%. The linear regression analysis reveals a significant R2 of 0.99 for the relationship between the population growth rate and agricultural growth rate at the 0.03 significance level, as well as a significant R2 of 0.58 for the relationship between agricultural growth rate and barren land reduction rate. A comparison of the district's vegetation and bareness indices reveals a 16.8% increase in vegetation and a 13.4% decrease in bareness, with the latter change mainly occurring in the south of the district, towards lesser Cholistan Correlation coefficients between vegetation and the bareness index were 0.83 in 1996 and 0.91 in 2020. As a consequence of considerable alterations in land use, the natural environment and arid ecosystem of the study area are deteriorating. This study can act as a template for local stakeholders aiming to enhance land use planning in the district by identifying areas that are most vulnerable to changes in land use.

Introduction

According to the United Nations Convention to Combat Desertification, desertification refers to land degeneration which occurs in arid, semi-arid and dry sub-humid regions because of different factors including ecological shifts and human conduct (UNCCD, 2017). The 2.7 billion inhabitants of drylands face severe social and ecological consequences from desertification while drylands occupy more than 41% of Earth's surface (Cherlet et al., 2018). Soil degradation through this process causes land to become non-productive thus diminishing fertility while reducing biodiversity and making populations more vulnerable. Sustainable land management together with overgrazing, deforestation, water scarcity, and climate change in addition to changing rainfall patterns create multiple desertification causes. Desertification creates multiple ecological and socio-economic impacts that affect food access and disrupts both local habitats and compels people living from natural resources to migrate. Different monitoring systems must be developed because effective desertification management requires precise tools for mapping land use and land cover transformations throughout time. Legal and scientific institutions have made geo-spatial technology essential due to its RS and GIS components. Scientists can study extensive inaccessible regions through high precision and dependable detection and visual analysis of spatial-temporal changes with these technologies (Lambin et al., 2003). An additional definition of desertification as the decline in a region's biological potential, which can ultimately lead to the desertification of fertile lands. When the precipitation level falls below what is necessary to sustain vegetation, the soil loses its vitality, leading to degradation (Kassas, 1995).

In fact, the United Nations Environment Programme (UNEP) explains desertification as the degradation or destruction of arid, semi-arid, and dry sub-humid environments primarily due to human activity. The change of fertile land, e.g., arable lands or cattle lands, into deserts is known to humanity under the name of land degradation. This phenomenon of the occurrence of land degradation is typically brought about by improper drainage, extensive irrigation, and water mismanagement (Kassas, 1995). Signs of land degradation could be a decrease in the productivity of the rangeland, the reduction of fertility in the soil and loss of biodiversity due to unsustainable land use patterns (Kassas et al., 1991).

Desertification has been identified as one major result of the changing global climate. Droughts, which are a common natural disaster, are now becoming more frequent due to climate changed are main by the increased global temperatures and the decreasing precipitation patterns (Kassas, 1995). Additionally, human generated activities such as deforestation, overgrazing, urban expansion, and poor water resource management also play a significant role in speeding up the process of desertification (Ouma & Ogallo, 2007). Bath's research (1999) on the desertification in sudia Arabia showed that relentless overgrazing was the primary cause of the reduction of rangeland productivity. The increased rainfall and high temperatures caused by the climate change have caused desertification in many areas leading to more than half a billion people losing their livelihoods as well as forcing them to migrate to other areas in search of better living conditions (Ouma & Ogallo, 2007).

Human has always been changing the Earth’s surface by taking care of their basic needs for food, clothes, and houses. Unfortunately, the consequences of such action are now visible in the deterioration of the environment. Change of land cover, and land use (LCLU) on our planet is a factor defining the global, regional, and local scales of this activity and is, in turn, driven by a number of forces like biophysical, institutional, technical, and economic ones. In developing regions, particularly in dry and semi-arid zones, LCLU change is most often a result of rapid population growth, which leads to the increase of the need for services like housing, agriculture,

and energy (Sharma et al., 2018; Liu et al., 2020). The conversion and utilization of natural resources have, as a result, enlarged over temporal and spatial scales (Alawamy et al., 2020; Bullock et al., 2021; Lin et al., 2020). It is increasingly becoming clear that Earth's natural resources are being destroyed and used up. Remote sensing presents us with a very useful way to monitor land cover land use change. Satellite data is being widely used as it is reliable and consistent over space and time. These data are obtained from multispectral passive sensors that are onboard earth orbiting satellites and other non-stationary or moving platforms. In particular, the use of high-resolution Landsat images with more than 4 decades of history and a 30-meter resolution has become essential. Landsat series instruments e.g., Landsat 5 TM, Landsat 7 ETM+ and Landsat 8 OLI have been stage marked for their performance and hence are the best known examples of this category (Fichera et al., 2012; Mohajane et al., 2018). Initially, the land use cover was determined by human analysts through visual evaluations of color, shape, tone, texture, and pattern (Phiri & Morgenroth, 2017). However, as the technology improved, digital image classification using different algorithms was the trend. One of the most popular algorithms e.g., maximum likelihood (ML) classifier, unsupervised and supervised classification (Clark et al., 2004). The definition of a change in LCLU is the one where several instances of such phenomena occur in a period when these events are observed. The process of change detection includes different steps, the most important ones being the selection of field data, which are used to train the algorithm, the choice of the algorithm, verification of the classified data accuracy, and comparison of different time periods' thus classified outputs (Ayele et al.,2018; Du et al., 2014; Tewabe & Fentahun, 2020). The rate of land cover conversion and the degree of the same are two of the most frequently used measures to determine the size of the transformation that has taken the place of the old scene (Tiamgne et al., 2021). One of the very well-liked band indexes known as the Normalized Difference Vegetation Index (NDVI) is often used for assessing the healthiness of vegetation, Normalized Difference Built-up Index (NDBI) for quantifying the urban region, and Normalized Difference Bareness Index (NDBaI) for pointing the barren land (Alawamy et al., 2020; Hussain et al., 2020; Kumar et al., 2021; Zhou et al., 2014).

NDVI, which is computed from the near-infrared (NIR) and red bands of Landsat, offers an accurate indication of vegetation vitality and biomass (Bhatta charjee et al., 2021; Morawitz et al., 2006). Kumar et al. (2021) have also developed an improved version based on the shortwave infrared bands called the NDSI index. Other indices such as Normalized Difference Soil Index (NDSI) and Bare Soil Index (BSI) are additionally utilized for the purpose of identifying areas without vegetation (Nguyen et al., 2021; Zhou et al., 2014). NDBaI, presented by Zhao and Chen (2005), is the most notable for separating no disturbance areas and is proven to be very useful especially in the arid areas (Hadeel et al., 2010; Nguyen et al., 2021). The different image band index technique was effective in changes detection of certain land features with the NDVI differencing approach being the one used for the same procedure. As a result, the use of band index differencing and the application of supervised classification provide a strong platform for the quantification and visualization of LCLU changes in terms of magnitude, direction, and rate (Alam et al., 2020). In our case, these approaches have been implemented to identify land cover changes using NDVI and NDBaI in our research area.

Urbanization, agriculture expansion, and climate change have been the main causes of dramatic and significant land cover/land use (LCLU) changes in Pakistan. Some examples of these changes have been reported in the studies of Hassan et al. (2016) in Islamabad. This current research, however, takes into account Bahawalpur District in southern Punjab, which is a parched land and an environmentally sensitive area that has gone under significant LCLU changes such as the growth of urban and agricultural sectors and a dramatic reduction in the natural habitat, etc. To the best of our knowledge, there are not many studies or none of them have been developed on this

topic through the utilization of NDVI and NDBaI difference image indices and those studies that exist may be focused on specific areas of the district.

(1) To statistically analyze the dynamics of change rates among various land use types through different indices?

(2) To evaluate 25 years of LCLU change using supervised maximum likelihood classification based on Landsat data.

Study area

Cholistan is located in the Great Desert, the world's seventh-largest desert, which stretches along the southern boundary of Pakistan's Punjab province (Rao et al., 1989). Covering approximately 26,000 square kilometres, the Cholistan Desert lies between 27°42′ and 29°45′ North, and 69°52′ and 75°24′ East (Arshad et al., 2007), at an average elevation of about 112 metres above sea level (Ali et al., 2009). As the climate changed, monsoon winds shifted away from the region, reducing precipitation and gradually transforming the area into a desert (Leopold, 1963). Rainfall is low and sporadic, averaging just 100–250 mm annually. The wettest months are typically during summer (July–September) and winter (January–March) (Arshad et al., 2006). During summer, the desert becomes a Death Valley, with extreme conditions due to high temperatures, low humidity, strong winds, and a high evaporation rate (Akram et al., 1986) making it the most barren and desolate part of the region. It includes both Lesser Cholistan the vegetation primarily consists of xeromorphic species that are well adapted to harsh conditions such as extreme dryness, high salinity, elevated temperatures, and nutrient deficiency (Naz et al., 2010). Cholistan, the district's desert area, makes up more than two-thirds of the total land area,

Map 1.1: Location of the study area: Cholistan Desert, Pakistan.

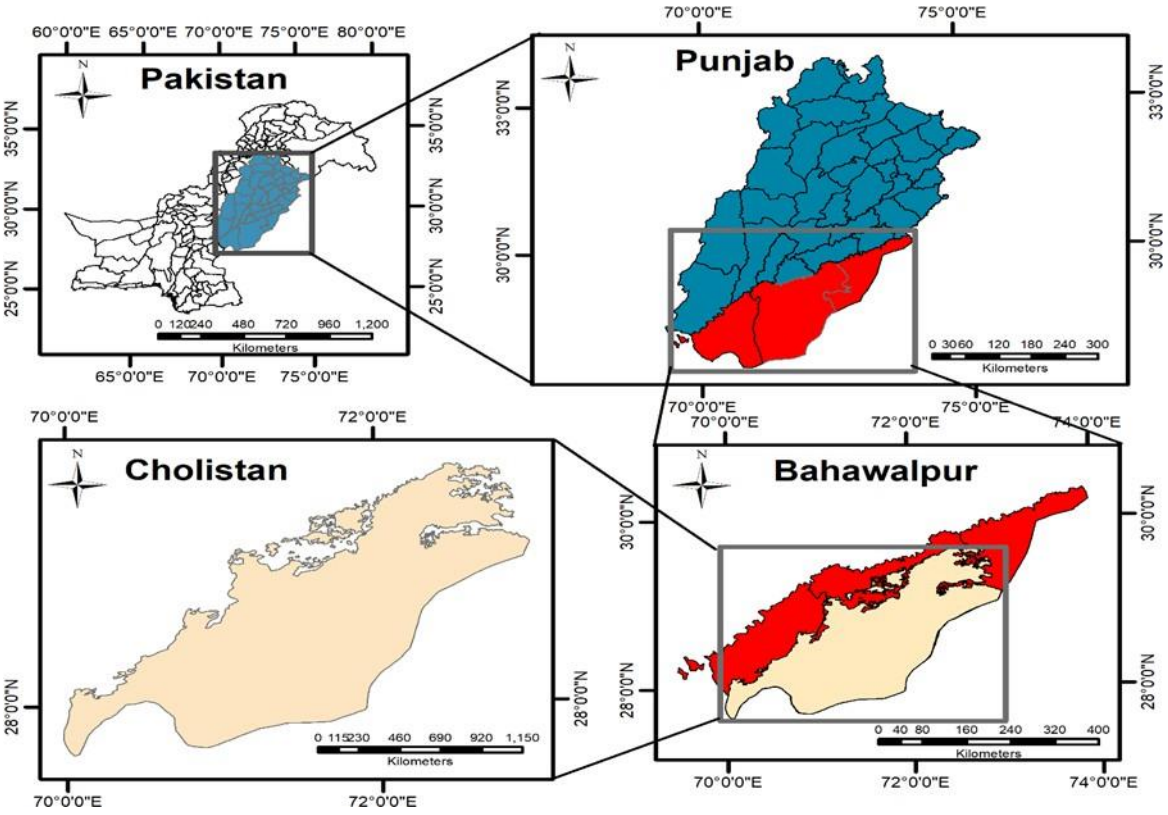

The desert stretches from the northern Bahawalnagar District to the southern Rahim Yar Khan District, located to the south and east of the irrigated tract (PCO, 1998). All mosaic images used in this research contributed to the shape file of the study area. The satellite images were geo-referenced using the UTM Zone 43N projection and the WGS 1984 datum. The year 2020 was used as the reference image during the geo referencing process, which also included images from 1996, 2002, 2008, and 2014. For enhanced visual analysis, edge detection and image sharpening techniques were applied.

Material and Method

This study employs remote sensing-based change detection techniques to analyze land cover/land use (LCLU) dynamics in the Cholistan Desert, Pakistan. Maximum likelihood supervised classification is applied to Landsat images, followed by annual dynamic rate of change analysis. NDVI, TGSI, and NDBaI indices are used to detect LCLU changes, considering the dominance of vegetation and barren land. Regression modeling assesses the relationship between land use change and population growth.

Image Acquisition & Preprocessing

Five multi-date cloud-free Landsat 5 TM and two Landsat 8 OLI images (1996–2020) were obtained from USGS (30m resolution) and processed in ERDAS Imagine 14. Preprocessing included atmospheric and geometric corrections, TOA reflectance conversion, and image enhancement. Geo referencing was done using UTM 43N projection with 2020 as the reference image.

Image Classification

LCLU classification scheme was developed based on physiographical conditions. Maximum likelihood classification (MLC) was applied to classify water, rangeland, vegetation, and barren land. Training data was sourced from historical imagery, field surveys, and census reports. Classification accuracy was evaluated using histograms, statistical means, and contingency matrices.

Accuracy Assessment

Classification accuracy was validated using an error matrix, computing overall accuracy and kappa coefficient. GPS-based field surveys collected 85 ground control points (GCPs). Google Earth imagery assisted in verification. 30% of GCPs were from unchanged areas.
Change Detection using Band Indices

NDVI (NIR/Red), NDBaI (SWIR/TIR), and TGSI (soil grain content indicator) were employed to analyze LCLU dynamics. These indices were validated through field surveys and regression modeling. All processing, classification, and accuracy assessments were performed in ERDAS Imagine 14.

Band Index-Based Change Detection

Normalized Difference Vegetation Index (NDVI), Normalized Difference Built-up Index (NDBaI), and Topsoil Grain Size Index (TGSI) were used for land cover change detection.

Equations:

- **NDVI** = (NIR - RED) / (NIR + RED)
- **NDBaI** = (SWIR - TIR) / (SWIR + TIR)
- **TGSI** = (Red - Blue) / (Red + Green + Blue)

NDVI values range from -1 to +1, where negative values indicate water, near-zero represents barren land, and positive values indicate vegetation. NDBaI highlights built-up areas, and TGSI differentiates soil grain sizes.

Change Detection & Analysis
Change detection was performed using multi-date NDVI and NDBaI images by computing:

- **ΔNDVI** = NDVI(2020) - NDVI(1996)
- **ΔNDBaI** = NDBaI(2020) - NDBaI(1996)

The dynamic rate of change (%) for land use was calculated as:

LuA(i+n)−LuA(i)n×LuA(i)×100\frac{LuA(i+n) - LuA(i)}{n \times LuA(i)} \times 100
where LuA represents land use area and n is the time interval.
Statistical Analysis
Linear regression in SPSS assessed the correlation between land use change and population growth:
y=a+bXy = a + bX
where yy is the predicted variable, XX is land use change rate, and RR (Pearson correlation) measures relationship strength. ANOVA determined model significance at p<0.05p < 0.05.

Results and Discussion

Land Use Dynamics (1996–2020)

Table 1.2 presents the accuracy assessment of land use classification, while Table 1.3 quantifies the area coverage of each land use type. Built-up land expanded from 215 sq. km (0.8%) in 1996 to 813 sq. km (3.2%) in 2020. Agricultural land increased from 3,239 sq. km (13%) in 2020 to 5,747 sq. km (23%) in 2020. The forest area grew marginally from 84 sq. km (0.3%) in 1996 to 115 sq. km in 2020. Water bodies fluctuated but increased overall from 58 sq. km in 1996 to 187 sq. km in 2020. Barren land declined significantly from 21,028 sq. km (85%) in 1996 to 17,531 sq. km (70%) in 2020. Fallow and other land uses varied between 0.8% and 1.7% over the study period.

Change Detection Analysis

This data shows changes in land utilization patterns during 1996 to 2020 which displays information about both land size in hectares and proportional area distribution from a total land mass of 2,970,714 hectares. Barren Land maintained its position as the dominant land use during the entire period because it consistently held most of the area while its portion declined from 97% in 1996 to 92% in 2020 showing a slow transformation of deserted territories into alternative land uses.

Other land categories and range land use expanded significantly throughout the twenty-four-year period from their initial 1% in 1996 to their final value of 6% in 2020. The trend of vegetation cover over time showed first a decrease from 1996 to 2002 followed by an increase with a total growth from 47,617 ha (2%) in 1996 to 59,048 ha (2%) in 2020. The data implies that the efforts of vegetation restoration and reforestation have been minimal but promising.

The analysis of water bodies demonstrated low variability because their size began at 5,015 ha (0%) during 1996 but reached its highest point at 26,766 ha (1%) in 2002 and returned to 3,096 ha (0%) by 2020. Liquid assets have decreased because of limited water availability and changes in climate patterns as well as improper water management. The land usage analysis demonstrates slow yet constant changes with barren land areas reducing while both rangeland and vegetation areas expanding throughout the 24-year period.

Table 1.1: Producer's, user's, and overall accuracy of classified images

Land use/years	Water		Vegetation		Range Land & Others		Barren Land		Overall accuracy
	P %	U %	P %	U %	P %	U %	P %	U %	
1996	100	100	100	99.8	98.8	96.4	99.5	100	98
2002	100	99.6	100	100	99.4	98.5	100	100	99
2008	100	100	100	100	99.5	99.7	100	100	99
2014	100	95.7	100	100	94.3	94.3	99.7	99.8	97
2020	100	100	100	100	98.8	98.8	100	100	99

Table 1.2: Area coverage (Hectares) and percentage share by each land use after classification

Land use categories	1996		2002		2008		2014		2020	
	Area (ha)	Area (%)	Area (ha)	Area (%)	Area (ha)	Area (%)	Area (ha)	Area (%)	Area (ha)	Area (%)
Water	5015	0%	26766	1%	4435	0%	4525	0%	3096	0%
Vegetation	47617	2%	22644	1%	67830	2%	33444	1%	59048	2%
Range Land & Other	43774	1%	77917	3%	107288	4%	106679	4%	171600	6%
Barren Land	2874308	97%	2843387	96%	2791162	94%	2826066	95%	2736970	92%
Total	2970714	100%	2970714	100%	2970714	100%	2970714	100%	2970714	100%

The classified land use maps from 1996 to 2020 indicate a clear trend of increasing vegetation cover and decreasing barren land in the Cholistan region. Over the years, vegetation has expanded, particularly along water bodies and in previously barren areas, suggesting afforestation and agricultural development. Water bodies have shown fluctuations, indicating possible changes in rainfall patterns, groundwater usage, or water management strategies. The steady decline in barren land suggests ongoing land conversion for agricultural and range land purposes, driven by population growth and increasing demand for arable land. If these trends persist, the landscape in the coming decades is likely to witness further vegetation expansion, a continued decline in barren land, and potential growth in water bodies if sustainable water management practices are adopted.

However, unplanned urbanization and excessive land conversion may pose environmental challenges, necessitating strategic conservation efforts to maintain ecological balance in the region.

Map 1.2: Land use thematic maps of each selected year from supervised classification

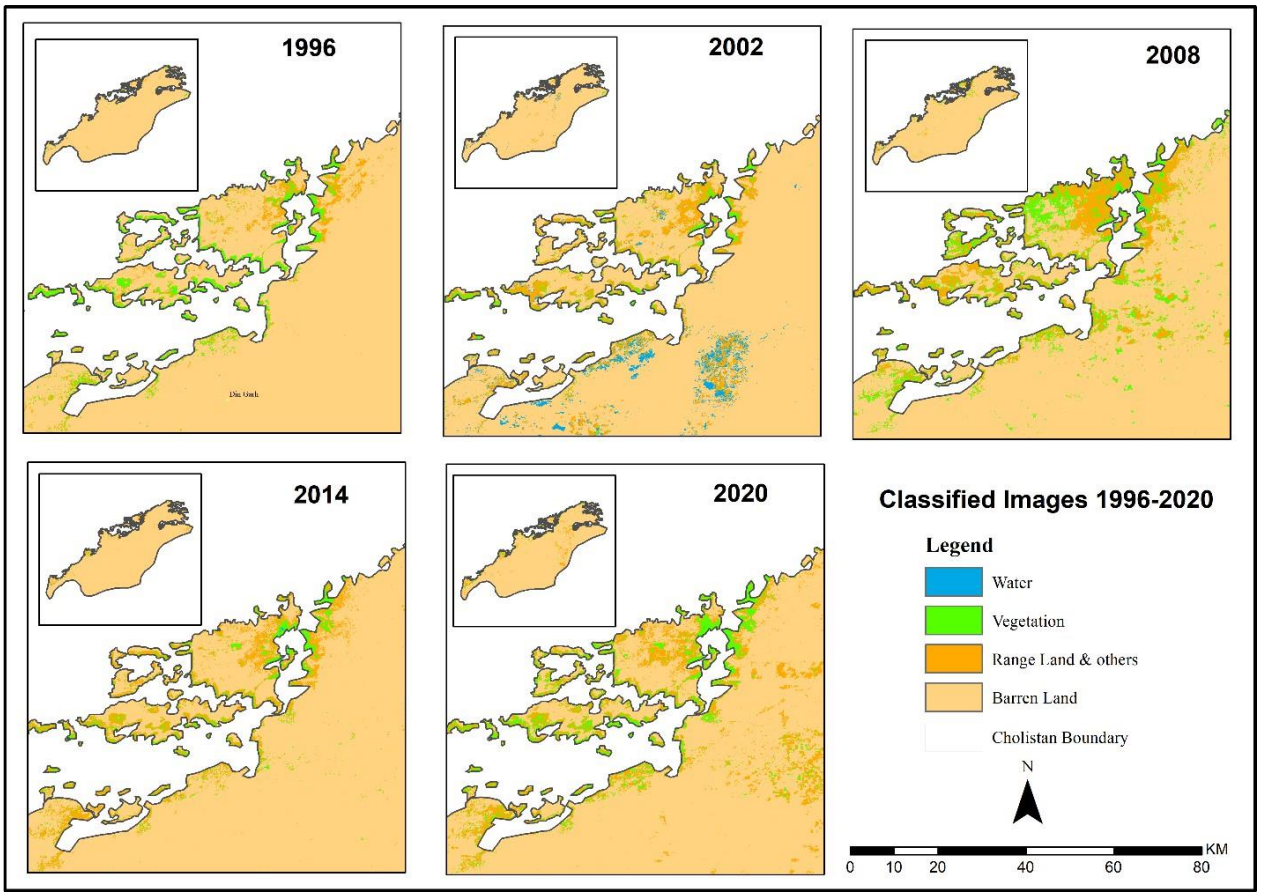

Table 1.3: Area, percent change, and dynamic annual change rate by each land use

	1996-2002		2002-2008		2008-2014		2014-2020	
Land use category	Change area (Hectares)	%Age change	Change area (Hectares)	%Age change	Change area (Hectares)	%Age change	Change area (Hectares)	%Age change
Water	21751	0.73	-22331	-0.75	90	0.003	-1429	-0.04
Vegetation	-24973	-0.84	45186	1.5	-34386	-1.1	25604	0..8
Range Land & Others	34143	1.1	29371	0.9	-609	-0.02	64921	2.1
Barren Land	-30921	-10.4	-52225	-1.7	34904	1.17	-89096	-2.9

The table presents land use changes across four time periods (1996–2002, 2002–2008, 2008–2014, and 2014–2020) in terms of area (hectares) and percentage change. The table shows the changes in land use categories over four time periods (1996–2002, 2002–2008, 2008–2014, and 2014–2020) in terms of both area (hectares) and percentage change. It provides insight into how different types of land cover have expanded or contracted over time. The Water category experienced a significant increase of 21,751 hectares (0.73%) between 1996 and 2002, possibly due to improved water storage or increased rainfall during that period. However, this gain was reversed in the next interval (2002–2008), with a sharp decline of 22,331 hectares (-0.75%), followed by relatively minor fluctuations in later periods—a small gain of 90 hectares (0.003%) from 2008–2014 and a

reduction of 1,429 hectares (-0.04%) from 2014–2020.Vegetation showed dynamic changes. It decreased by 24,973 hectares (-0.84%) between 1996 and 2002, possibly due to deforestation or land degradation. However, it recovered strongly between 2002 and 2008 with an increase of 45,186 hectares (1.5%), then declined again by 34,386 hectares (-1.1%) in the next period. From 2014 to 2020, vegetation increased once more by 25,604 hectares (0.8%), suggesting cycles of loss and regeneration, likely influenced by both human activity and environmental conditions.

The percentage of land used for Range Land & Other purposes expanded consistently from 1996 to 2008. The first period brought a 34,143-hectare (1.1%) increase while the following period displayed another 29,371-hectare (0.9%) growth. During the time between 2008 and 2014 the total area covered by range Land & Other uses showed a small reduction of 609 hectares before experiencing significant growth of 64,921 hectares in the following period.

The Barren Land territory suffered continuous reduction through two time periods together decreasing by 83,146 hectares (-2.7%) during 1996–2002 and 2002–2008. The area covered by Barren Land demonstrated a minor growth between 2008–2014 to reach a total of 34,904 hectares (1.17%) yet it suffered its biggest reduction to 89,096 hectares (-2.9%) across the 2014–2020 period. The extensive decline demonstrates that barren areas are gradually converting into functional terrains used for vegetation and rangelands.

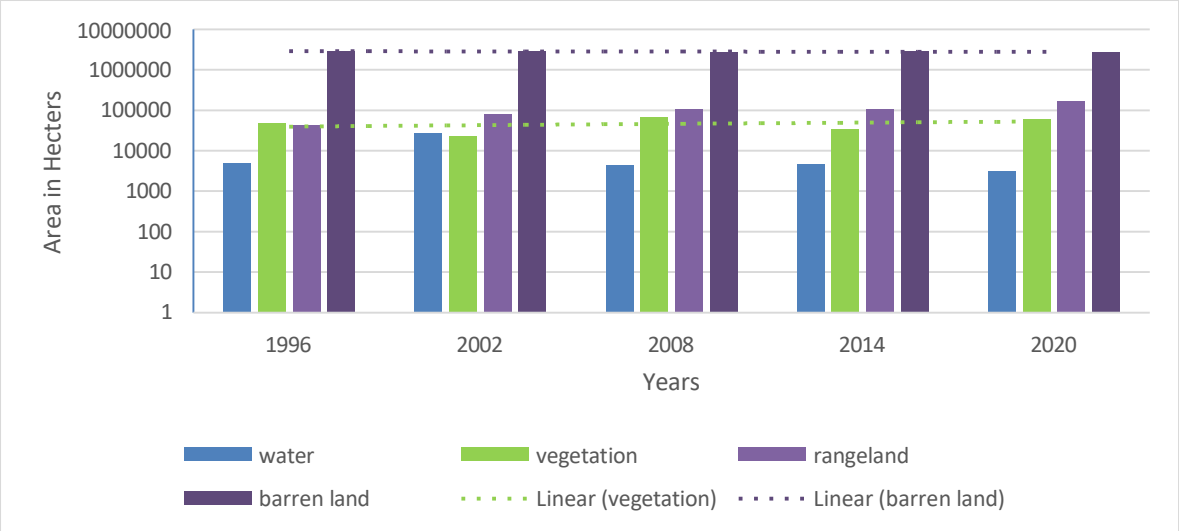

Fig.1.1: Area percent change by each land use class in respective time periods

The data indicates a major decreasing pattern of barren land and increasing patterns of rangeland and vegetation while water resources remain unstable. Natural environmental factors and active land management operations which focus on sustainability seem to explain these observed patterns.

The visual is an illustration of a change in the use of the earth's surface. On the one hand, the graph reflects a decrease in the area of land left unutilized while other land uses (rangeland and water) exhibit almost the same state of affairs or minor rising. It may imply that the unused land is being developed by other sectors of the economy, such as the city's expansion, or the building of the forest and agriculture sectors. The lower curve in the barren land is a clear sign that land

untouched by humans or unproductive land has been transformed into useful forms which has brought a difference in the ecological landscape.

Map 1.3: NDBaI From 1996-2020

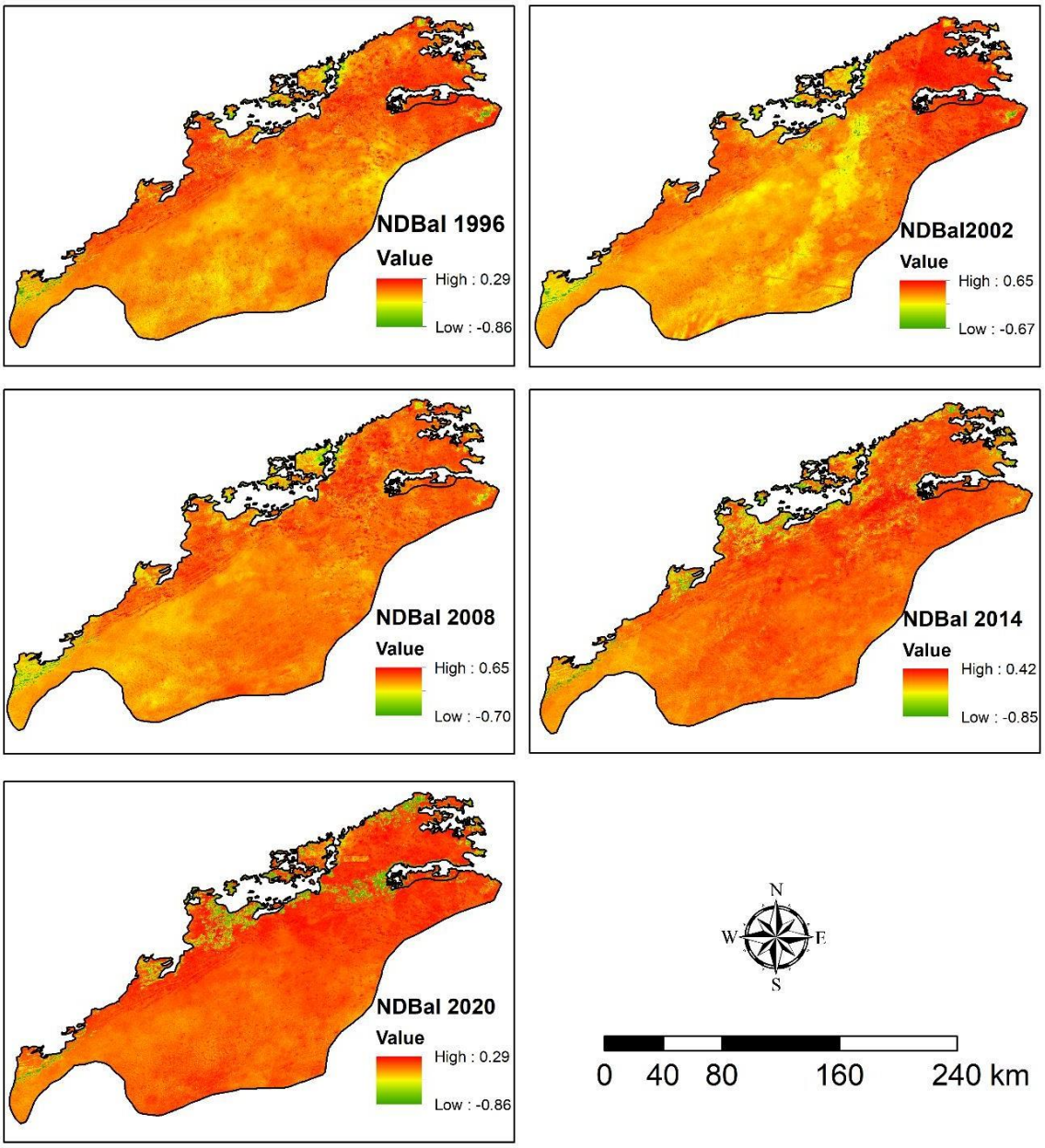

The image is about the information that was captured for the years 1996, 2002, 2008, 2014, and 2020 represented in each case, shown a range of "Value" with "High" and "Low" limits. The High figures fluctuate between 0.29 and 0.65, while the low ones fluctuate around from -0.66 to -0.86, showing the changes in trends What was the factor that contributed to this query? The trend shows that the highest High value occurred in 2002 and 2008 (0.65), whereas the lowest Low value wasb registered in 2020 (-0.86). Environmental modifications, altered land use, or other factors are quite likely the reasons behind such changes over the 24-year interval. The text's aim and the exact situation are not that clear without the added data, but it sounds like the author tries to find time-related fluctuations in a certain metric.

Map 1.4: NDVI From 1996-2020

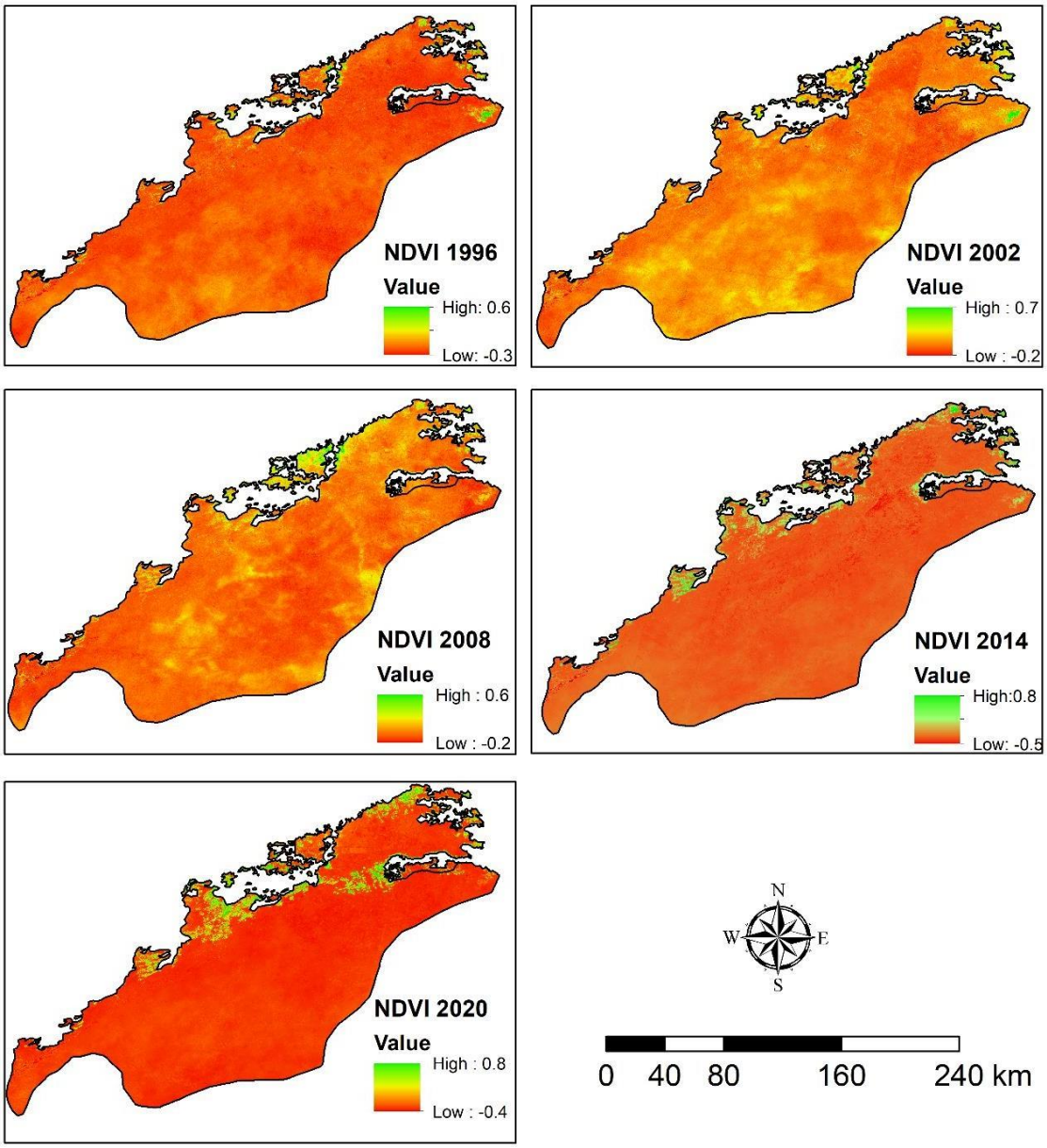

The visual is a graphic of the NDVI (Normalized Difference Vegetation Index) measurements for the years 1996, 2002, 2008, 2014, and 2020, and their highest as well as their lowest values. NDVI is a leading index to determine the healthiness of the flora, having values ranging from -1 to 1, where bigger positive numbers (e.g., 0.6-0.8) mean a healthier vegetation, while the negative ones (e.g., -0.9 to -0.2) frequently denote water, snow, or barren land. The highest NDVI values in the history of the series experienced the peak in 2014 and then further growth in 2020 (0.8), which expressed lush vegetation. Still, the lowest point (-0.9 in 2014) might be a result of harsh conditions like drought or the accumulation of snow cover. The bar scale under the graph (0-240 km) can be assumed to be the geographical extent of the study area, e.g. monitoring a certain place for changes in vegetation. The trend shows variety in the condition of the plants. Some years reported improvements, e.g., 2002, 2014 & 2020, and some reported declines, e.g., 1996 to 2008. This series is fit for studying the influence of weather change on local economies, shifts in the way lands are used, or the dynamics of the ecosystem throughout the years.

Map 1.5: TGSI From 1996-2020

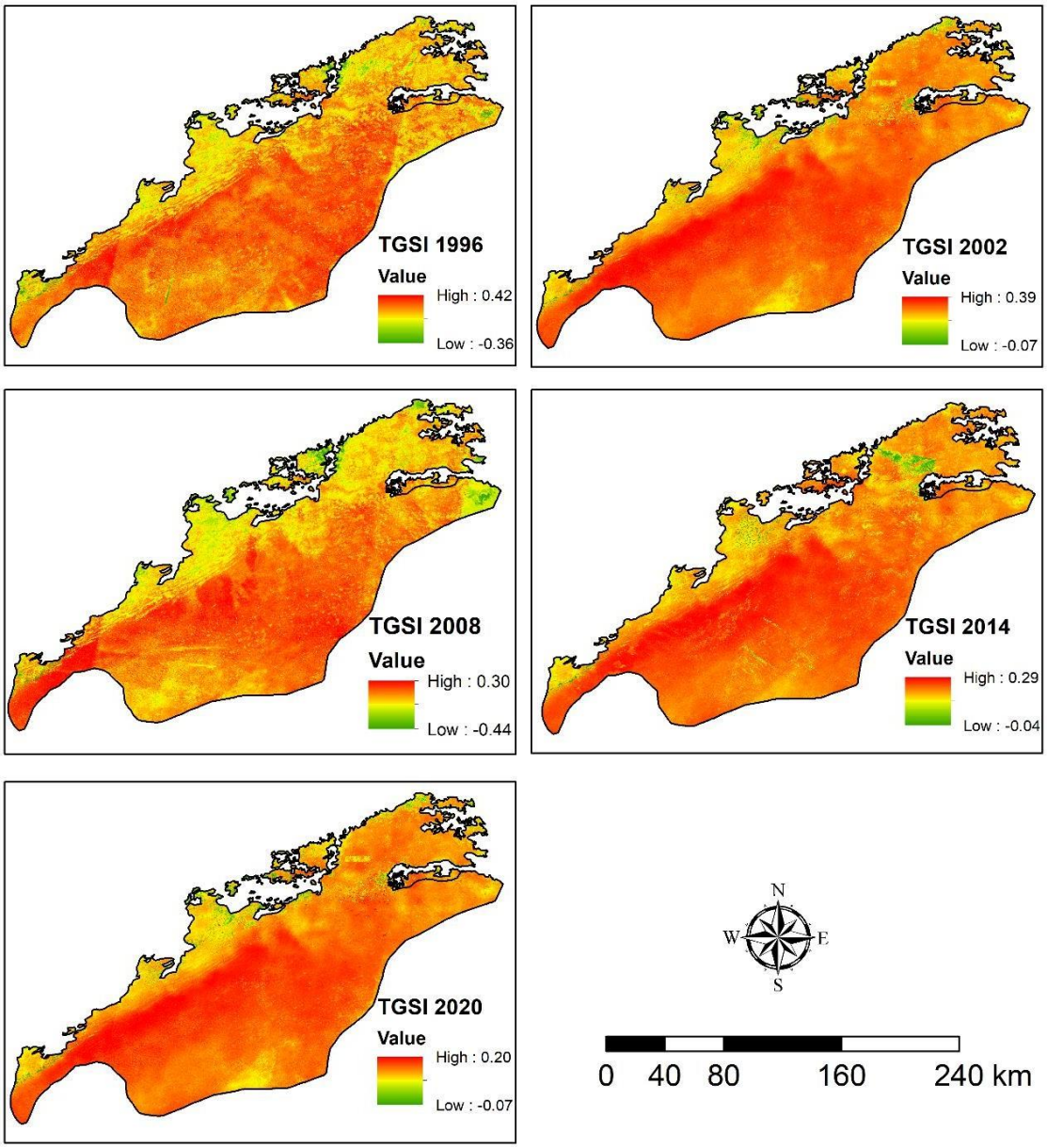

The image presents a long-term dataset labeled TGSI (Top Grain Soil Index)**,** which likely measures soil quality or health, spanning from 1996 to 2020**.** The index records annual high and low values**,** where higher values (closer to 1) indicate better soil conditions, and lower or negative values suggest degradation or stress.

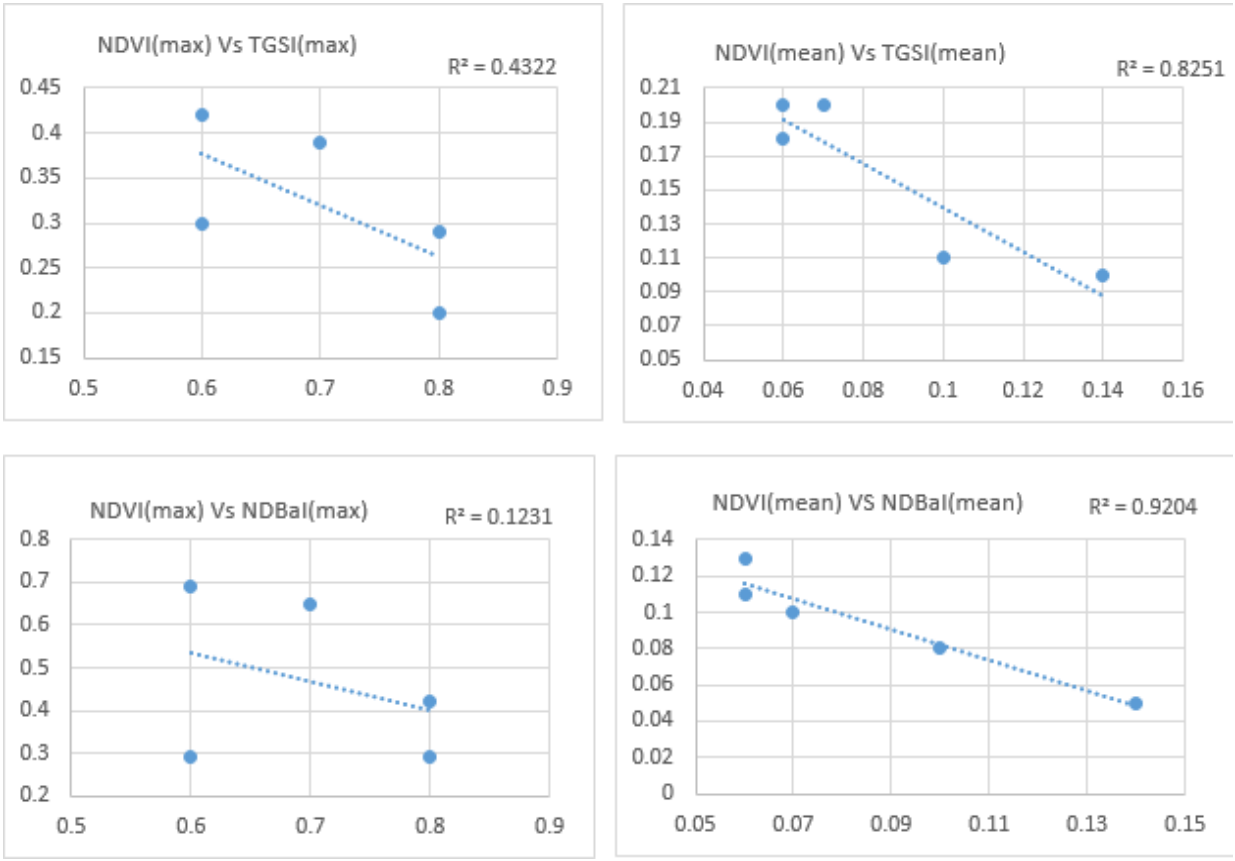

Fig. 1.2: Linear regression between land use growth rate dynamic

Figure 1.2 presents' four scatter plots with linear regression lines, showing the relationship between NDVI (Normalized Difference Vegetation Index) and two key land surface indicators: TGSI (Topsoil Grain Size Index) and NDBaI (Normalized Difference Built-up Index). The R^2 values indicate the strength of correlation between variables. In the top-left graph, a moderate negative correlation ($R^2 = 0.4322$) is observed between NDVI (max) and TGSI (max), suggesting that areas with coarser topsoil tend to have lower vegetation density. The top-right graph shows a strong negative correlation ($R^2 = 0.8251$) between NDVI (mean) and TGSI (mean), indicating a consistent inverse relationship between average vegetation cover and fine-grained topsoil composition. This suggests that vegetation is more abundant in areas with lower TGSI values (i.e., more fine-textured soils). In the bottom-left graph, a weak negative correlation ($R^2 = 0.1231$) is observed between NDVI (max) and NDBaI (max), implying that maximum vegetation cover is only slightly affected by built-up land areas. However, the bottom-right graph displays a very strong negative correlation ($R^2 = 0.9204$) between NDVI (mean) and NDBaI (mean), indicating that increased built-up activity is strongly associated with reduced average vegetation cover. Overall, the figure suggests that both soil texture and urban development significantly influence vegetation dynamics, with mean values offering stronger correlations than maximum values. The results highlight the importance of monitoring these indicators to understand and manage land use change effectively.

Map 1.6: NDBaI, NDVI & TGSI change detection from 1996-2020

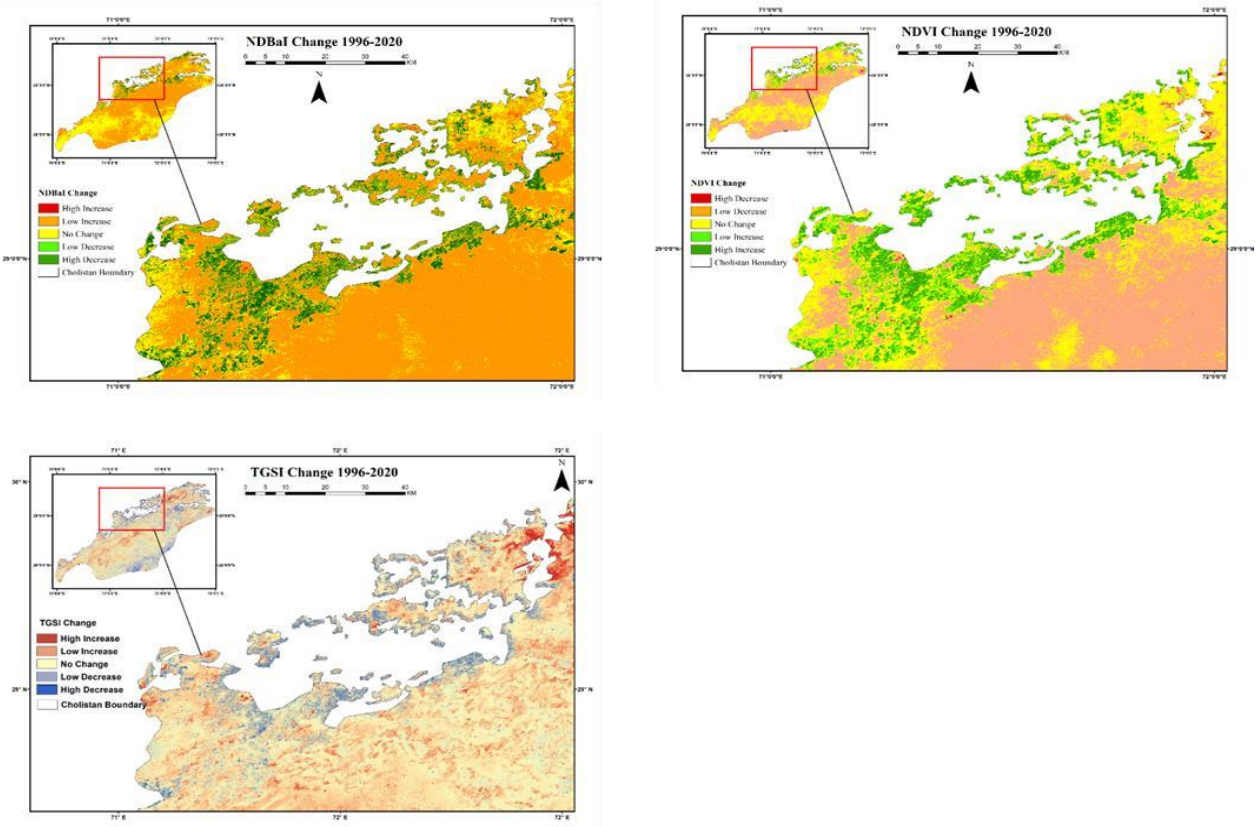

Table 1.4: Change Detection from 1996-2020

Area In Hectares	1996-2002	2002-2008	2008-2014	2014-2020
water	2070	-2650	90	-1429
vegetation	-24973	45186	-34386	127126
Rrangeland & others	34143	-29371	-609	63479
Barren land	-11240	-71906	34904	-189176

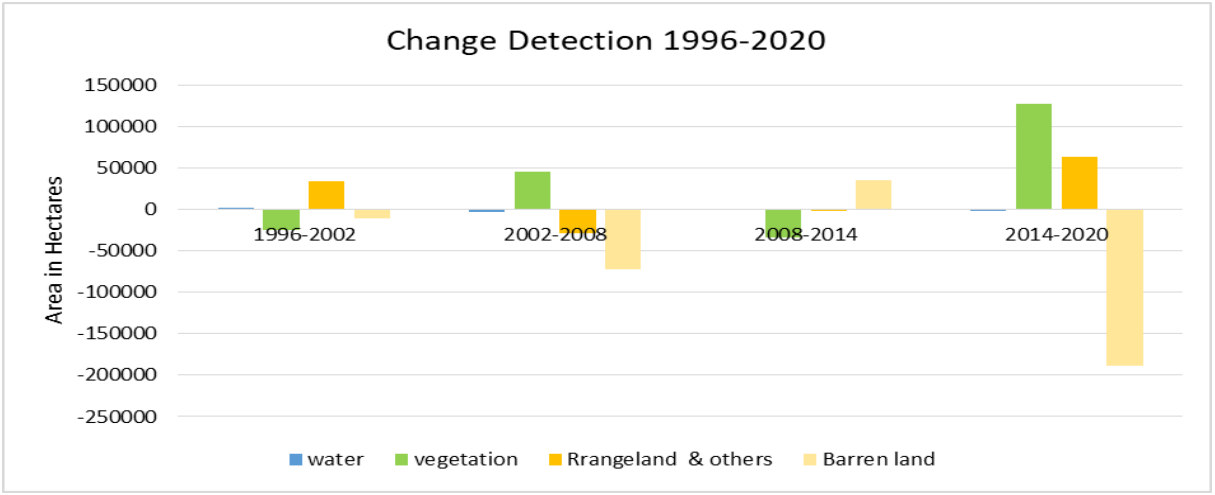

Figure 1.3: Change Detection from 1996 to 2020

The complete statistics of all images chosen for the current study from 1996 to 2020 intervals are shown in the above figure. The statistics display the area (in hectares) corresponding to each image. The other aspect is a change that took place during this specified six-year period. Figure 1.3 illustrates the changes in land cover, highlighting that water has increased while vegetation and rangeland have decreased, and other land covers have risen. Barren land also decreased from the 1996 to 2020 images. Between 2002 and 2008, the water area diminished, while vegetation and rangeland expanded; however, barren land also decreased. Between 2008 and 2014, the water area experienced a slight increase, vegetation decreased, rangeland and other areas decreased, and barren land also decreased. Between 2014 and 2020, the water area experienced a slight decrease, while vegetation and rangeland increased; however, barren land saw a significant reduction.

Change Detection through NDVI, NDBaI and TGSI analysis

Results obtained from maximum likelihood classification indicate an expansion of agriculture and a reduction of barren land in the study area, which is further confirmed by analyzing NDVI, NDBaI, and TGSI of the study area as shown in Map 1.6.

Table 1.5 : Mean, Maximum value of indices in study area

NDVI	**min**	**max**	**Mean**	**Std.dev**
1996	-0.3	0.6	0.07	0.02
2002	-0.2	0.7	0.06	0.01
2008	-0.2	0.6	0.06	0.01
2014	-0.5	0.8	0.10	0.06
2020	-0.4	0.8	0.14	0.12
NDBaI	**min**	**max**	**Mean**	**Std.dev**
1996	-0.86	0.29	0.10	0.05
2002	-0.67	0.65	0.11	0.04
2008	-0.70	0.65	0.13	0.03
2014	-0.85	0.42	0.08	0.04
2020	-0.86	0.29	0.05	0.10
TGSI	**min**	**max**	**Mean**	**Std.dev**
1996	-0.36	0.42	0.20	0.01
2002	-0.07	0.39	0.20	0.01
2008	-0.44	0.30	0.18	0.06
2014	-0.04	0.29	0.11	0.01
2020	-0.07	0.20	0.10	0.01

The vegetation, top grain soil, and barren land indices presented in Table 1.5 indicate that the land use pattern in the study area has undergone significant spatial-temporal changes. NDVI reached its highest values of 0.6 in 1996, 0.7 in 2002, 0.6 again in 2008, 0.7 in 2014 and 0.8 in year 2020. The average NDVI increased from 0.07 to 0.14 between 2010 and 2020, signaling a healthy and expanding vegetation cover. TGSI reached its highest values of 0.42 and 0.39 in the years 1996 and 2002, respectively. Table 1.5 shows that the maximum value was attained as plant cover increased and TGSI values decreased. Assessed at 0.30 in 2008, 0.29 in 2014, and 0.20 in 2020. The mean TGSI decreased from 0.20 to 0.10. It demonstrates that the amount of barren land has decreased, resulting in a reduction of top-grain soil reflectivity. The reflection of the highest barren land reported a maximum NDBaI value of 0.29% in 1996, which rose to 0.65% in 2002 and 2008. It decreased to 0.42% in 2014 and further declined to 0.29% in 2020. The average NDBaI value drops from 0.10 in 1996 to 0.05 in 2020.

Table 1.6: Summary Statistics of NDVI, NDBaI and TGSI in the study area

Index	Change type	Area sq. km	Percentage
NDVI	High Decrease	18170	0.2
	Low Decrease	4637266	62.6
	No Change	2290977	30.9
	Low Increase	196097	2.6
	High Increase	270087	3.6
NDBaI	High Decrease	20522	2.8
	Low Decrease	24914	3.4
	No Change	233516	31.5
	Low Increase	461346	62.2
	High Increase	961	0.1
TGSI	High Decrease	16693	2.3
	Low Decrease	145471	19.6
	No Change	339271	45.8
	Low Increase	214281	28.9
	High Increase	25541	3.4

According to NDVI change detection in Table 1.6 and Map 1.5, an area of 18170 sq.km (0.2%) experienced a significant decrease in vegetation, while an area of 4637206 sq.km (62.6%) saw a minor decrease, indicating that vegetation was reduced in this portion. Additionally, 2290977 sq.km (30.9%) exhibited no changes throughout the study period. In the study area, 196,097 sq. km (or 2.6% of the total area) is characterized by low-increase vegetation. However, the area of 270087 sq.km or 3.6% shows a significant increase in vegetation. The percentage of barren land that quickly turns into agricultural land is 3.6%. The change detection of NDBaI in map 1.5 and Table 1.6 indicates that an area of 20,522 sq. km (2.8% of the total) has been reduced and transformed into agricultural land, while bareness decreased relatively modestly over a span of three decades in an area measuring 24,914 sq. km (3.4%). Additionally, an unchanged area in the Cholistan desert amounted to 233,516 sq. km (31.5%). In the study area, 461,346 sq. km (62.2%) exhibit low increases in bareness, while 961 sq. km (0.1%) show an increase in bareness. in the Study area, while 20,056 sq. km, or 80% of the area, predominantly consisting of Cholistan desert, has remained unchanged for three decades. The TGSI change detection in Table 1.6 and Map 1.5 indicates that a reduction of 16,693 sq. km (2.3%) of barren land occurred as it was converted into agricultural land, resulting in a significant decrease in TGSI. An area of 145,471 sq. km (19.6%) fell into the category of low decrease, while 339,271 sq. km (45.8%) remained constant within the study area. Conversely, a reduction of 214,281 sq. km (28.9%) in bareness led to an increase in TGSI, and an area of 25,541 sq. km (3.4%) experienced a significant increase. Analysis of change detection reveals that there have been two significant changes in land use within the study area: arable land has increased, while undeveloped areas have decreased. Our study reveals a new pattern of land use transformation compared to other studies conducted in Pakistan at the Study area level. However, our research indicates that desert wastelands have a fertile potential for agricultural expansion. In lower Cholistan, vacant land is being transformed into farmland, particularly for wheat cultivation, which poses an increasing threat to the area's arid or desert ecology. Consequently, the alteration of land use due to population growth and socioeconomic advancement throughout the region is emerging as a significant factor in biodiversity loss, climate change intensification, and soil quality degradation (Samie et al. 2020). Although many changes in land use have occurred in the area, indigenous farmers possess extensive knowledge about it. We utilize this information in our research to corroborate the land-use patterns noted.

References

1. Alawamy, J. S., Balasundram, S. K., Hanif, A. H. M., & Sung, C. T. B. (2020). Detecting and analyzing land use and land cover changes in the region of Al-Jabal Al-Akhdar, Libya using time-series Landsat data from 1985 to 2017. Sustainability, 12(11), 4490.
2. Bath, J. (1999). Monitoring desertification in Saudi Arabia using remote sensing. Applied Geography, 19(4), 363–381.
3. Bullock, E. L., Woodcock, C. E., Souza, C., & Olofsson, P. (2021). Satellite-based estimates reveal widespread forest degradation in the Amazon. Global Change Biology, 27(2), 356–365.
4. Cherlet, M., Hutchinson, C., Reynolds, J., Hill, J., Sommer, S., & von Maltitz, G. (2018). *World atlas of desertification* (3rd ed.). Publication Office of the European Union.
5. Chughtai, M. U., Butt, M. J., & Waqas, A. (2021). Land use/land cover change assessment using remote sensing and GIS: A case study of Rawalpindi District. Environmental Earth Sciences, 80(6), 1–14.
6. Fichera, C. R., Modica, G., & Pollino, M. (2012). Land cover classification and change-detection analysis using multi-temporal remote sensed imagery and landscape metrics. European Journal of Remote Sensing, 45(1), 1–18.
7. Jensen, J. R. (1996). Introductory digital image processing: A remote sensing perspective (2nd ed.). Prentice Hall.
8. Jingan, S., Jiupai, N., Chaofu, W., & Deti, X. (2005). Land use change and its corresponding ecological responses: A review. Journal of Geographical Sciences, 15(3), 305–328.
9. Kassas, M. (1995). Desertification: A general review. Journal of Arid Environments, 30(2), 115–128.
10. Kassas, M., & others. (1991). Ecosystem degradation: A global problem. Ambio, 20(1), 2–10.
11. Kuma, P. K., Suresh, M., & Suganthi, J. (2022). Land use and land cover change detection using remote sensing and GIS techniques: A case study of Coimbatore District, India.
12. Lambin, E. F., Geist, H. J., & Lepers, E. (2003). *Dynamics of land-use and land-cover change in tropical regions*. Annual Review of Environment and Resources, 28(1), 205–241.
13. Lin, Y. P., Hong, N. M., Wu, P. J., Wu, C. F., & Verburg, P. H. (2007). Impacts of land use change scenarios on hydrology and land use patterns in the Wu-Tu watershed in Northern Taiwan. Landscape and Urban Planning, 80(1-2), 111–126.
14. Liu, X., Chen, X., Hua, K., Wang, Y., Wang, P., Han, X., Ye, J., & Wen, S. (2018). Effects of land use change on ecosystem services in arid area ecological migration. Chinese Geographical Science, 28(5), 894–906.
15. Mohajane, M., Mhammdi, N., & El Gharbaoui, A. (2018). Land use/land cover change detection and prediction in the high basin of the Oum Er Rbia River (Morocco) using Landsat images: 1987–2017. Remote Sensing Applications: Society and Environment, 13, 361–374.
16. Ouma, G., & Ogallo, L. (2007). Degradation of the environment: A case study of the Machakos District, Kenya. Environmental Monitoring and Assessment, 132(1-3), 273–281.
17. Phiri, D., & Morgenroth, J. (2017). Developments in Landsat land cover classification methods: A review. Remote Sensing, 9(9), 967.
18. Rimal, B., Sharma, R., Kunwar, R., Keshtkar, H., Stork, N. E., Rijal, S., & Baral, H. (2020). Effects of land use and land cover change on ecosystem services in the Koshi River Basin, Eastern Nepal. Ecosystem Services, 38, 100963.

19. Sharma, G., Sharma, L. K., & Sharma, K. C. (2019). Assessment of land use change and its effect on soil carbon stock using multitemporal satellite data in semiarid region of Rajasthan, India. Ecological Processes, 8(1), 1–13.
20. United Nations Conference on Desertification (UNCOD). (1977). Desertification: Its causes and consequences.
21. United Nations Convention to Combat Desertification (UNCCD). (2017). *The Global Land Outlook – First Edition.*
22. Wulder, M. A., Roy, D. P., Radeloff, V. C., Loveland, T. R., Anderson, M. C., Johnson, D. M., ... & Zhu, Z. (2019). Fifty years of Landsat science and impacts. Remote Sensing of Environment, 225, 127–147.